Environmental Science
Water Research & Technology

PAPER

Cite this: *Environ. Sci.: Water Res. Technol.*, 2019, **5**, 1072

Long-term performance evaluation of an anoxic sulfur oxidizing moving bed biofilm reactor under nitrate limited conditions†

Ramita Khanongnuch, *[a] Francesco Di Capua, [c] Aino-Maija Lakaniemi, [a] Eldon R. Rene [b] and Piet N. L. Lens [ab]

Received 16th March 2019,
Accepted 24th April 2019

DOI: 10.1039/c9ew00220k

rsc.li/es-water

An anoxic sulfur-oxidizing moving bed biofilm reactor (MBBR) treating sulfur and nitrate-contaminated synthetic wastewater was monitored for 306 days under feed nitrogen-to-sulfur (N/S) molar ratios of 0.5, 0.3 and 0.1. Thiosulfate ($S_2O_3^{2-}$) removal efficiencies (RE) exceeding 98% were observed at a N/S ratio of 0.5 and a $S_2O_3^{2-}$ loading rate of 0.9 g $S_2O_3^{2-}$–S L^{-1} d^{-1}, whereas a RE of 82.3 (±2.6)% and 37.7 (±3.4)% were observed at N/S ratios of 0.3 and 0.1, respectively. Complete nitrate (NO_3^-) removal was obtained at all tested N/S ratios. A comparison of the kinetic parameters of the MBBR biomass under the same stoichiometric conditions (N/S ratio of 0.5) revealed a 1.3-fold increase of the maximum specific rate of $S_2O_3^{2-}$ oxidation (r_{max}) and a 30-fold increase of the affinity constant for $S_2O_3^{2-}$ (K_s) compared to those observed after long-term NO_3^- limitation (N/S ratio of 0.1). The MBBR showed optimal resilience to NO_3^- limitation as the $S_2O_3^{2-}$ RE recovered from 37.3% to 94.1% within two days after increasing the N/S ratio from 0.1 to 0.5. Based on PCR-DGGE analysis, sulfur-oxidizing nitrate-reducing bacteria, *i.e. Thiobacillus* sp. and *Sulfuritalea* sp., dominated in the MBBR biofilm during the entire study.

Water impact

Reduced sulfur compounds and nitrate-contaminated wastewater harm the environment and public health. This work presents an effective MBBR process for the simultaneous removal of sulfur and nitrogen pollutants prior to discharging to surface waters. Sulfur-oxidizing biofilm in the MBBR showed resilience to nitrate fluctuations (*i.e.* limitation) in the influent, which is useful for practical applications.

1. Introduction

Wastewaters such as pig manure, tannery effluents and pulp and paper processing effluents generally contain elevated concentrations of sulfur in the form of thiosulfate ($S_2O_3^{2-}$), polythionate ($S_nO_6^{2-}$), elemental sulfur (S^0), sulfite (SO_3^{2-}) and sulfate (SO_4^{2-}), which are reduced to hydrogen sulfide (H_2S) during anaerobic digestion.[1] The presence of sulfide species (H_2S, HS^- and S^{2-}) in gaseous and wastewater streams is highly detrimental due to their ability to cause corrosion and adverse effects in the environment.[2]

The removal of sulfur contaminants such as H_2S and $S_2O_3^{2-}$ using nitrate (NO_3^-) as the electron acceptor has gained increasing interest since reduced sulfur compounds and NO_3^- can be simultaneously removed from waste streams by a single anaerobic process.[3–7] The operation of anoxic sulfur-oxidizing bioreactors entails the use of a highly soluble electron acceptor (*i.e.* NO_3^-) and eliminates oxygen gas–liquid-biofilm mass transfer limitations commonly experienced in aerobic systems.[8] Moreover, the operation of anoxic bioreactors has low environmental impacts and operational costs if nitrified wastewater or NO_3^--containing wastewater is provided as a source of NO_3^-.[9,10] The reaction involved in the anoxic oxidation of $S_2O_3^{2-}$ and sulfide in the presence of NO_3^- is described by eqn (1) and (2), respectively:[11]

$$S_2O_3^{2-} + 1.16NO_3^- + 0.124H_2O + 0.035CO_2 + 0.519HCO_3^- + 0.11NH_4^+ \rightarrow 2SO_4^{2-} + 0.578N_2 + 0.110C_5H_7O_2N + 0.435H^+ \quad (1)$$

$$HS^- + 1.23NO_3^- + 0.573H^+ + 0.438HCO_3^- + 0.027CO_2 + 0.093NH_4^+ \rightarrow SO_4^{2-} + 0.614N_2 + 0.866H_2O + 0.093C_5H_7O_2N \quad (2)$$

[a] *Tampere University, Faculty of Engineering and Natural Sciences, P.O. Box 541, FI-33014 Tampere, Finland. E-mail: ramita.khanongnuch@tuni.fi*
[b] *UNESCO-IHE Institute for Water Education, Westvest 7, 2611 AX Delft, The Netherlands*
[c] *Department of Civil, Architectural and Environmental Engineering, University of Napoli Federico II, 80125 Napoli, Italy*

† Electronic supplementary information (ESI) available. See DOI: 10.1039/c9ew00220k

Moving bed biofilm reactors (MBBR) have been widely used for the treatment of domestic and industrial wastewaters due to their effective biomass retention.[12–14] However, few studies focused on the operation of anoxic MBBRs for treating sulfur contaminated wastewaters. Full-scale sulfur-oxidizing bioreactors may experience fluctuations in the influent NO_3^- concentration as well as an unexpected increase or decrease of sulfur loading, which can lead to severe NO_3^- limitation in the system. Furthermore, when the NO_3^- and nitrite (NO_2^-) concentrations in the influent wastewater are insufficient to sustain the process, a NO_3^- source (*e.g.*, $NaNO_3$, KNO_3, $Ca(NO_3)_2$) can be supplied externally to maintain the process efficiency.[15] Dosing must be strictly controlled to minimize the addition of chemicals and the operational costs. As a result, it is important to evaluate the long-term performance of an anoxic MBBR under NO_3^- limitation as well as the response and resilience capacity of the sulfur-oxidizing nitrate-reducing (SO-NR) MBBR biofilm to such fluctuations. Process control evaluation and microbial community analysis are important to better understand the operational and biological variables determining the performance of the system. In this study, the long-term performance and microbial community evolution were evaluated in an anoxic sulfur-oxidizing MBBR at different N/S ratios (0.5 and 0.3 and 0.1) for 306 days.

2. Materials and methods

2.1. Inoculum source and synthetic wastewater composition

The MBBR was inoculated with biofilm-coated granular activated carbon (GAC) collected from a laboratory-scale fluidized-bed reactor (FBR) previously operated to study the effects of temperature, hydraulic retention time (HRT) and pH on thiosulfate-driven denitrification.[16,17] The microbial community of the biofilm-coated GAC was dominated by sulfur-oxidizing bacteria, *i.e. Thiobacillus denitrificans* and *Thiobacillus thioparus*. The GAC-attached biomass had total solid (TS) and volatile solid (VS) concentrations of 23.0 (±1.5) and 17.3 (±1.3) g L^{-1} of GAC, respectively. The VS/TS ratio was approximately 0.75–0.76.

The synthetic wastewater used in this study contained 200 mg $S_2O_3^{2-}$–S L^{-1} (added as $Na_2S_2O_3{\cdot}5H_2O$), 10–45 mg NO_3^-–N L^{-1} (added as KNO_3), 1 g L^{-1} of $NaHCO_3$ and nutrients (mg L^{-1}) as follows: KH_2PO_4 (200), NH_4Cl (100), $MgSO_4{\cdot}7H_2O$ (80), $FeSO_4{\cdot}7H_2O$ (2) and 0.2 mL L^{-1} of a trace element solution as described by Zou *et al.*[6] The pH of the synthetic wastewater was adjusted to 7.0 using 37% HCl. $S_2O_3^{2-}$ was used as the representative reduced sulfur compound due to its ease of handling and stability at circumneutral pH.[11,18]

2.2. Experimental set-up and operation

The MBBR used in this study was made of glass and had a working volume of 0.825 L (Fig. 1). The MBBR was filled with 350 (±5) pieces of Kaldnes-K1 carriers [specific surface area: 500 m^2 m^{-3}, effective area: 410 mm^2 per piece, density: 0.95 g cm^{-3}, diameter × height: 9 × 7 mm], corresponding to a 40% filling ratio. The influent was fed to the MBBR at a flow rate of 4.0 L d^{-1} (Masterflex® Easy Load II L/S driven by Masterflex® L/S, Cole-Parmer, USA), corresponding to a theoretical hydraulic retention time (HRT) of 5 h. Mixing was provided with a Heidolph RZR 2052 mechanical stirrer (Heidolph Instruments GmbH & Co. KG, Germany) operated at a speed of 65 rpm. The MBBR was operated at room temperature (20 ± 2) °C.

Initially, the MBBR was filled with 180 pieces of K1 carriers (51% of total carriers) and 10 mL of biofilm-coated GAC taken from a previously operated FBR for thiosulfate-driven denitrification[17] as inoculum. Then the synthetic wastewater was fed to the MBBR up to 800 mL. The MBBR was purged with N_2 for 15–20 min to ensure the anoxic conditions and operated in batch mode for 14 days. Batch operation was stopped when the $S_2O_3^{2-}$ and NO_3^- RE exceeded 90% and biofilm formation was visually observed on the K1 carriers.

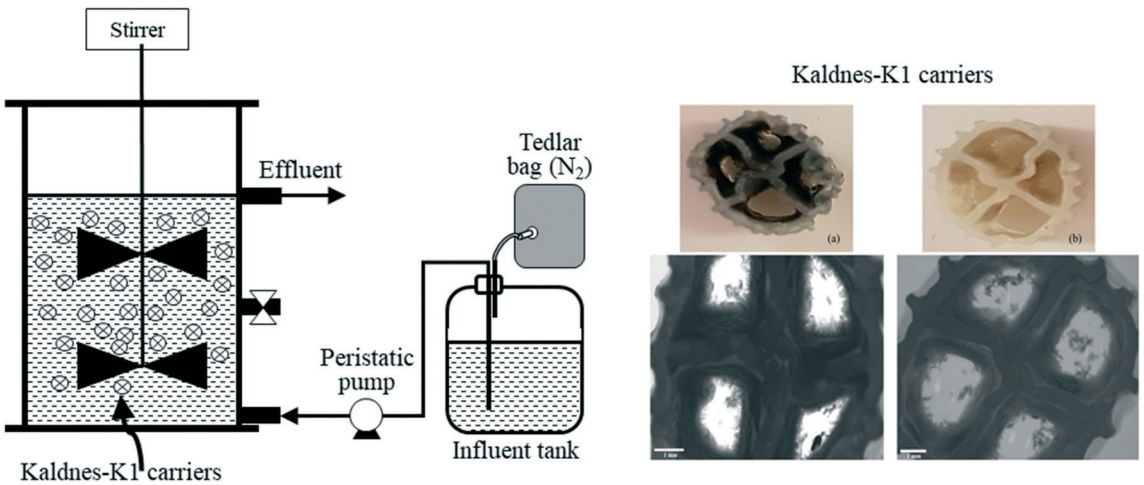

Fig. 1 Schematic representation the MBBR used in this study, including a photograph of the two different biofilm types attached to the Kaldnes-K1 carriers: (a) thick-dark brown biofilm, and (b) thin-light brown biofilm.

Afterwards, the GAC was completely removed and 170 pieces of K1 carriers were added to the MBBR prior to starting continuous operation.

Continuous MBBR operation (306 days) was divided into five experimental periods (Table 1). During the entire experiment, the influent $S_2O_3^{2-}$ concentration was kept constant at ~200 mg $S_2O_3^{2-}$–S L^{-1}, corresponding to an inlet $S_2O_3^{2-}$ loading rate of 0.91 (±0.05) kg $S_2O_3^{2-}$–S m^{-3} d^{-1}, while the influent NO_3^- concentration was varied between 10.6 and 40.5 mg NO_3^-–N L^{-1} in order to adjust the N/S ratio (Table 1). During period I (days 0–45), the microbial community in the MBBR was acclimated to continuous operation at a stoichiometric N/S ratio of 0.5 (Table 1) to ensure that the biofilm formed on the K1 carriers could sustain the simultaneous removal of $S_2O_3^{2-}$ and NO_3^-. The dissolved oxygen (DO) concentration in the MBBR was 0.87 (±0.31) mg L^{-1}. In period II (days 46–115), the operational conditions were similar to period I but the DO concentration was reduced to 0.45 (±0.08) mg L^{-1} (Fig. 2a) as a N_2-filled Tedlar bag was connected to the top of the influent tank in order to reduce oxygen intrusion and maintain the anoxic conditions.

During period III (days 116–207), the MBBR was operated at a N/S ratio of 0.3, corresponding to an influent NO_3^- concentration of 28.7 (±1.7) mg NO_3^-–N L^{-1} and an inlet NO_3^- loading rate of 0.14 kg NO_3^-–N m^{-3} d^{-1}. In period IV (days 208–249), the influent NO_3^- concentration was decreased to 10.6 (±0.6) mg NO_3^-–N L^{-1}, corresponding to an inlet NO_3^- loading rate of 0.05 kg NO_3^-–N m^{-3} d^{-1}, and the MBBR operated at a N/S ratio of 0.1. During period V (days 250–306), an influent NO_3^- concentration of 39.4 (±1.5) mg NO_3^-–N L^{-1} (N/S ratio of 0.5) was used in order to investigate the MBBR potential to recover the $S_2O_3^{2-}$ RE after a 42 day operation under NO_3^- limited conditions (period IV).

The performance of the MBBR in each experimental period was evaluated under steady-state operating conditions. The steady-state condition was assumed when the relative standard deviation (% RSD) of the $S_2O_3^{2-}$ RE was ≤10%.

2.3. Batch kinetic bioassays

Batch bioassays were performed to determine the kinetic constants, *i.e.* the maximum specific rate of $S_2O_3^{2-}$ oxidation (r_{max}) and the affinities of the biofilm microorganisms to $S_2O_3^{2-}$ (K_s) and NO_3^- (K_n). Bioassays were performed in duplicate in 120 mL serum bottles with 60 mL headspace, and the medium solution (pH 7.0 ± 0.2) had the same composition as the synthetic wastewater used for the continuous MBBR operation. Biofilm-attached K1 carriers (9 pieces per bottle) were taken from the MBBR during steady-state conditions of operational periods II–V (days 117, 196, 244 and 305, respectively) and used as inoculum. The initial $S_2O_3^{2-}$ and NO_3^- concentrations used in these bioassays were as shown in Table 2. The bottles were purged with N_2 for 10 min and sealed with rubber septa and aluminum crimps to ensure anoxic conditions. Subsequently, the bottles were placed on a HS 501 horizontal shaker (IKA, USA) operated at 220 rpm and 20 (±2) °C. In this study, the simultaneous $S_2O_3^{2-}$-oxidizing NO_3^--reducing process was described using a Monod model (eqn (3)):

$$r_S = \frac{r_{max} \times S}{K_s + S} \times \frac{N}{K_n + N} \quad (3)$$

However, the simplified Monod model (eqn (4)) was used when the affinity constant for NO_3^- (K_n) was much smaller than the initial NO_3^- concentration (N).[19] This was the case for microbial biofilm samples taken from the MBBR during low N/S ratio conditions (N/S ratios of 0.3 and 0.1).

$$r_S = \frac{r_{max} \times S}{K_s + S} \quad (4)$$

where S and K_s are the concentration and affinity constant for $S_2O_3^{2-}$ (mg $S_2O_3^{2-}$–S L^{-1}), respectively; N and K_n are the concentration and affinity constant for NO_3^- (mg NO_3^-–N L^{-1}), respectively; and r_{max} is the maximum specific rate of $S_2O_3^{2-}$ oxidation (mg $S_2O_3^{2-}$–S g VS^{-1} h^{-1}).

2.4. Batch activity tests

Batch tests were performed in duplicate to study the SO-NR activity of the MBBR biomass by measuring the specific uptake rates of $S_2O_3^{2-}$ (STUR) and NO_3^- (SNUR) (Table S1†). On day 117 (period II), the tests were performed to evaluate the metabolic activity of the two different types of biofilm formed on the K1 carriers, *i.e.* thick-dark biofilm and thin-light biofilm. At the end of the experiment (day 306, period IV), batch tests were performed to evaluate the effect of three sequential feedings on the carrier-attached and suspended biomass. The second and third feeding of $S_2O_3^{2-}$ and NO_3^- were sequentially added to the batch bottles before they were almost completely consumed. The nutrient solution was as described for the kinetic bioassays. K1 carriers (5 pieces per bottle) were taken from the MBBR and directly added as inoculum to 60 mL serum bottles with 20 mL headspace.

Table 1 Conditions of the anoxic MBBR during the different operational periods

Period	Time (days)	DO concentration (mg L^{-1})	Feed N/S ratio (mol mol^{-1})	Influent $S_2O_3^{2-}$ (mg $S_2O_3^{2-}$–S L^{-1})	Influent NO_3^- (mg NO_3^-–N L^{-1})	Effluent pH
I	0–45	0.87 (±0.31)	0.5	199.0 (±26.1)	40.5 (±3.4)	7.11 (±0.25)
II	46–115	0.45 (±0.08)	0.5	185.7 (±4.7)	39.4 (±1.5)	6.82 (±0.13)
III	116–207	0.53 (±0.09)	0.3	194.1 (±12.4)	28.7 (±1.7)	7.12 (±0.12)
IV	208–249	0.52 (±0.9)	0.1	197.2 (±7.5)	10.6 (±0.6)	7.28 (±0.12)
V	250–306	0.54 (±0.8)	0.5	186.8 (±3.2)	39.6 (±1.4)	6.93 (±0.09)

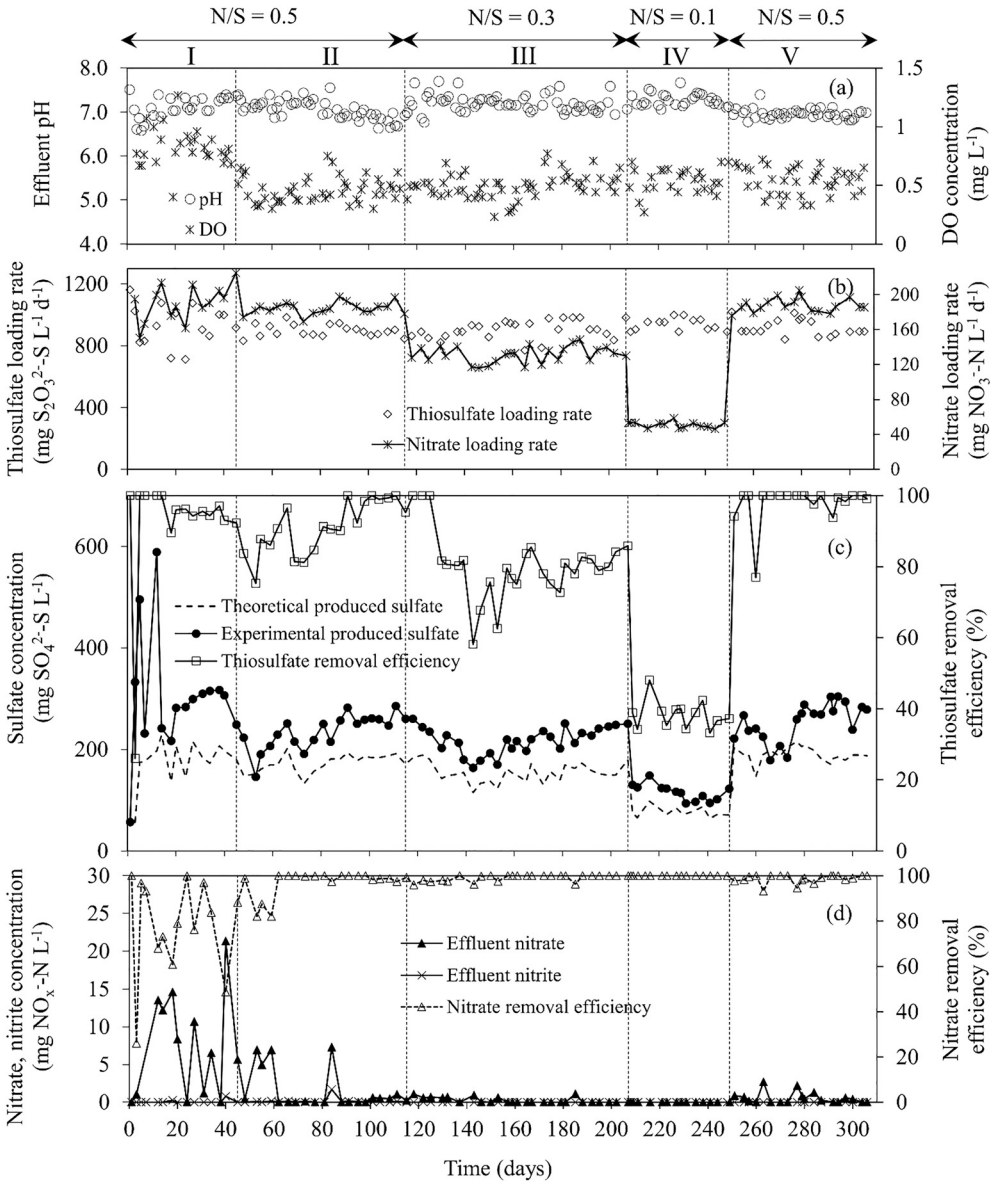

Fig. 2 Time course profiles of (a) effluent dissolve oxygen concentration and pH, (b) $S_2O_3^{2-}$ and NO_3^- loading rates, (c) $S_2O_3^{2-}$ removal efficiency and effluent SO_4^{2-} concentration, (d) effluent NO_3^- and NO_2^- concentrations and NO_3^- removal efficiency during MBBR operation. The dashed line in (c) indicates the theoretical SO_4^{2-} production based on eqn (1).

Table 2 Kinetic coefficients (Monod) of the attached biofilm collected from the MBBR during different operational periods

Period	N/S ratio (mol mol^{-1})	Biomass concentration (mg VS L^{-1})	Initial concentrations		Kinetic coefficients		
			$S_2O_3^{2-}$ (mg $S_2O_3^{2-}$–S L^{-1})	NO_3^- (mg NO_3^-–N L^{-1})	r_{max} (mg $S_2O_3^{2-}$–S g^{-1} VS h^{-1})	K_s (mg $S_2O_3^{2-}$–S L^{-1})	K_n (mg NO_3^-–N L^{-1})
II	0.5	495 (±105)	0, 6, 85, 160, 180, 300	0, 1, 15, 26, 36, 62	109.4	1.7	6.3
III	0.3	465 (±230)	0, 40, 80, 160, 270, 380	0, 6, 12, 24, 30, 50	113.1	67.0	—
IV	0.1	320 (±30)	0, 70, 130, 360, 480	0, 3, 6, 14, 20	69.2	109.3	—
V	0.5	490 (±200)	0, 35, 70, 200, 300, 420	0, 7, 15, 45, 62, 85	143.9	50.6	8.9

2.5. Residence time distribution (RTD) test

The RTD test for the MBBR, at a theoretical HRT of 5 h, was performed on day 307 to determine the hydrodynamic behavior of the MBBR using the pulse input method as described by Khanongnuch *et al.*[5] The procedure used to perform the RTD test and data analysis are described in Fogler.[20] The results obtained from the RTD test were used to determine the Peclet number (Pe_r) that describes the mixing characteristics of the MBBR as shown in eqn (5).

$$\frac{\sigma^2}{t_m^2} = \frac{2}{Pe_r} - \frac{2}{Pe_r^2}\left(1 - e^{-Pe_r}\right) \quad (5)$$

where σ^2 and t_m are the variance and mean residence time of the RTD, respectively.

2.6. Microbial community analysis

Two pieces of K1 carrier were taken during the steady-state operation of the MBBR in periods II (day 115), III (day 196), IV (day 242) and V (day 306). To obtain the bacterial cells from the carrier material, a biofilm-attached K1 carrier was immersed in 10 mL sterile Milli-Q water and sonicated for 2 min. The obtained solution was filtered through a Cyclopore track etched 0.2 μm membrane (Whatman, USA). Subsequently, the membranes with the retained biomass were stored at −20 °C for microbial community analysis by polymerase chain reaction denaturing gradient gel electrophoresis (PCR-DGGE). The DNA extraction was performed using a PowerSoil® DNA isolation kit (MO BIO Laboratories, Inc., USA) according to the manufacturer's instructions. PCR-DGGE analysis was performed according to the protocol described by Ahoranta *et al.*[21] The amplified DNA samples were sequenced by Macrogen Inc. (The Netherlands). The sequence data was edited using the Bioedit software (version 7.2.5, Ibis Biosciences, USA) and compared with the sequences available in the National Center for Biotechnology Information (NCBI) database.

2.7. Analytical techniques

The concentrations of $S_2O_3^{2-}$, SO_4^{2-}, NO_3^- and NO_2^- in the MBBR influent and effluent were measured by ion chromatography (IC) as described by Di Capua *et al.*[17] Liquid samples were filtered through 0.45 μm Chromafil Xtra PET-202125 membrane syringe filters (Macherey-Nagel, Germany) and stored at −20 °C prior to analysis. The DO concentration in the MBBR was measured with a HQ40d portable multimeter equipped with an Intellical™ LDO101 probe (HACH, USA). The influent and effluent pH of the MBBR were measured using a pH 3110 portable meter fitted with a SenTix 21 electrode (WTW, Germany). The pH of the liquid samples obtained from batch tests was measured using a pH 330i meter (WTW, Germany) fitted with a SlimTrode lab pH electrode (Hamilton, USA). Alkalinity was measured according to the procedure described in Standard methods.[22]

During MBBR operation (days 44, 60, 90, 114, 196, 242 and 306), two pieces of K1 carrier were collected to measure the total solids (TS) and volatile solids (VS) of the K1 carrier-attached biomass. Each piece of K1 carrier was added into a 15 mL Falcon tube containing 10 mL of deionized water and the biofilm was detached by manual shaking. The procedure was repeated until all the biomass was detached from the carrier. The solution containing the detached biomass was used for the determination of TS and VS contents of the carriers according to the same procedure for the volatile suspended solids (VSS) concentration in liquid samples given in Standard methods.[22] Elemental sulfur (S^0) was measured from K1 carriers collected on days 193, 240 and 300 using the modified cyanolysis method.[5]

2.8. Statistical analysis

A one-way analysis of variance (ANOVA) with Tukey's multiple comparison test was performed for data analysis using the Minitab 16 software (Minitab Inc., USA) to determine the statistical differences in each parameter during the steady-state operation of the MBBR. The significant difference was considered at 95% ($P \leq 0.05$). The kinetic constants of Monod (eqn (3) and (4)) were determined using the non-linear programming solver (fminsearch) in MATLAB® R2018b (MathWorks Inc., USA).

3. Results

3.1. MBBR performance at different N/S ratios

Fig. 2 shows the MBBR performance at different N/S ratio operations. During period I (days 0–44), the $S_2O_3^{2-}$ RE was 95.2 (±1.4)%, while the NO_3^- RE fluctuated between 48.7 and 100%, respectively. The effluent pH varied in the range of 6.86–7.36. During period II (N/S ratio of 0.5), the $S_2O_3^{2-}$ RE was 98.5 (±0.7)%. The effluent pH and alkalinity were 6.82 (±0.13) and 342 (±14) mg HCO_3^- L^{-1}, respectively. A NO_3^- RE higher than 99% was observed from day 60 onwards (Fig. 2d). A similar $S_2O_3^{2-}$ removal rate of 0.85 (±0.04) kg S m^{-3} d^{-1} was observed during periods I and II.

MBBR operation at N/S ratios below 0.5 resulted in lower $S_2O_3^{2-}$ removal rates and efficiencies than those observed in the first two operational periods. The $S_2O_3^{2-}$ RE was 82.3 (±2.6)% at a N/S ratio of 0.3 (period III) and 37.7 (±3.4)% at a N/S ratio of 0.1 (period IV), corresponding to $S_2O_3^{2-}$ removal rates of 0.62 (±0.04) and 0.38 (±0.01) kg S m^{-3} d^{-1}, respectively. The effluent pH and alkalinity were 7.12 (±0.17) and 393 (±15) mg HCO_3^- L^{-1} in period III and increased to 7.28 (±0.12) and 440 (±10) mg HCO_3^- L^{-1}, respectively, when the MBBR was operated at a N/S ratio of 0.1 (period IV) (Fig. 2a). The $S_2O_3^{2-}$ RE increased from 37.3% (day 249) to 94.1% (day 251) in two days after increasing the N/S ratio from 0.1 to 0.5 (period V). The $S_2O_3^{2-}$ RE further increased slightly during period V and reached 99.5 (±0.7)% at the end of the experiment (days 292–306), corresponding to a $S_2O_3^{2-}$ removal rate of 0.87 (±0.02) g S m^{-3} d^{-1}.

Fig. 2c shows the effluent SO_4^{2-} concentration profile in the MBBR at different N/S ratios tested. The highest effluent SO_4^{2-} concentration (302 ± 14 mg SO_4^{2-}–S L^{-1}) was observed during the acclimation phase (period I, N/S ratio of 0.5), while the lowest (105 ± 11 mg SO_4^{2-}–S L^{-1}) was observed during period IV (N/S ratio of 0.1). In periods II and V (N/S ratio of 0.5), similar effluent SO_4^{2-} concentrations were observed, *i.e.* 263 (±14) and 279 (±22) mg SO_4^{2-}–S L^{-1}, respectively. During period III (N/S ratio of 0.3), the effluent SO_4^{2-} concentration was 241 (±9) mg SO_4^{2-}–S L^{-1}.

3.2. Residence time distribution

The mean residence time (t_m) in the MBBR obtained from the RTD analysis was 4.43 h, while the theoretical HRT calculated based on the influent flow rate was 5 h. Regarding the dimensionless RTD function ($E(\Theta)$) (Fig. S1†), the normalized time (Θ) was defined as the RTD profile time (t) divided by t_m. Thus, at $\Theta = 1$ (the value of perfect completely mixed reactor) ($t = t_m = 4.43$ h), 64% of the tracer had left the reactor, corresponding to an accumulative profile ($F(\Theta)$) of 0.64 (Fig. S1†). The tracer completely left the MBBR within 22 h after the pulse injection. According to the mixing characteristics, the Peclet number (Pe_r) of 0 represents an ideal completely mixed reactor, whereas the value of an ideal plug flow is infinity (∞). In the present study, the hydrodynamic behavior of the MBBR ($Pe_r = 1.31$) was very close to that of an ideal completely mixed reactor, resulting in a uniform distribution of $S_2O_3^{2-}$ and NO_3^- in the reactor during the study.

3.3. Biofilm quantity, characteristic and viability during MBBR operation

The weight of the carrier-attached and suspended biomass in the MBBR during continuous operation was as shown in Fig. 3. The formation of thick-dark brown biofilm was observed on K1 carriers added prior to starting the 14 day batch mode operation (Fig. 1a), while the carriers added at the end of the batch mode operation were observed having thin-light brown biofilm (Fig. 1b). The thick-dark brown biofilm likely formed due to fine activated carbon particles attaching to the surface of K1 carriers.

The weight of the carrier-attached biomass with thick-dark brown biofilm was 1.20 (±0.14) mg VS per carrier on day 44 and gradually increased up to 2.17 (±0.15) mg VS per carrier on day 90 (period II, N/S ratio of 0.5). Afterwards, the biomass quantity remained relatively stable until the end of the experiment (day 306). The quantity of the carrier-attached biomass with thin-light brown biofilm was nearly constant in this study (0.88–1.28 mg VS per carrier), except in period IV (day 242) when the weight was only 0.35 (±0.14) mg VS per carrier (Fig. 3). The carrier-attached biomass with thick-dark brown and thin-light brown biofilm showed similar metabolic activities (STUR and SNUR) during period II (Table S1†).

Fig. 4 shows the activity of carrier-attached and suspended biomass during the sequential feedings of $S_2O_3^{2-}$ and NO_3^- in batch activity tests. After the first, second and third sequential feeding steps, the carrier-attached biomass showed a STUR and SNUR of 4.1–5.8 g $S_2O_3^{2-}$–S g VS d^{-1} and 0.84–1.81 g NO_3^-–N g VS d^{-1}, respectively (Fig. 4a, Table S1†). STUR and SNUR of the suspended biomass increased from 1.13 (±0.07) g $S_2O_3^{2-}$–S g VSS d^{-1} and 0.28 g NO_3^-–N g VS d^{-1} after the first feeding to 4.91 (±0.86) g $S_2O_3^{2-}$–S g VSS d^{-1} and 1.10 (±0.08) g NO_3^-–N g VS d^{-1} after the third feeding, respectively (Fig. 4b, Table S1†).

A positive correlation between biomass weight on K1 carriers and the S^0 concentration in the MBBR was observed on days 193, 240 and 300 (data not shown). The carriers with thick-dark biofilm (Fig. 1a) contained a higher amount of S^0 (33.5–76.6 μg per carrier) than those with thin-light biofilm (Fig. 1b) (8.2–14.6 μg per carrier).

3.4. Kinetic parameters of $S_2O_3^{2-}$ oxidation based on batch bioassays

The Monod model was successfully used to describe $S_2O_3^{2-}$ oxidation coupled to NO_3^- reduction at different N/S ratios during MBBR operation (Fig. 5). The highest r_{max} (144.0 mg $S_2O_3^{2-}$–S g^{-1} VS h^{-1}) was obtained with the biomass taken in period V (N/S ratio of 0.5) after 42 days of operation at severe NO_3^- limitations (N/S ratio 0.1, period IV), while similar r_{max} values (111.3 ± 1.8 mg $S_2O_3^{2-}$–S g^{-1} VS h^{-1}) were obtained in periods II (N/S ratio of 0.5) and III (N/S ratio of 0.3) (Table 2). The lowest biofilm affinity for $S_2O_3^{2-}$ (K_s = 1.70 mg $S_2O_3^{2-}$–S L^{-1}) was observed in bioassays performed during period II (N/S ratio of 0.5), while the highest K_s value (109.43 mg $S_2O_3^{2-}$–S L^{-1}) was observed during period IV (N/S ratio of 0.1).

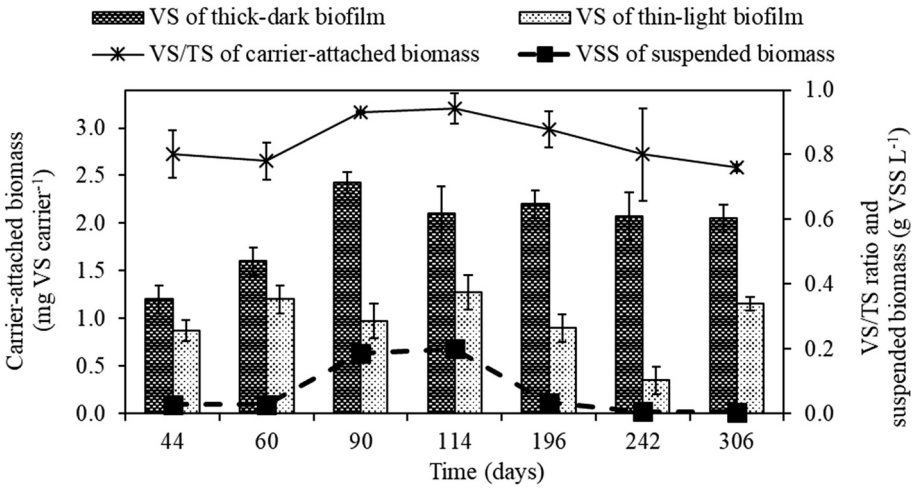

Fig. 3 Biomass evolution in the MBBR during operational periods I (days 44, 60, 90 and 114), II (day 196), III (day 242) and IV (day 306).

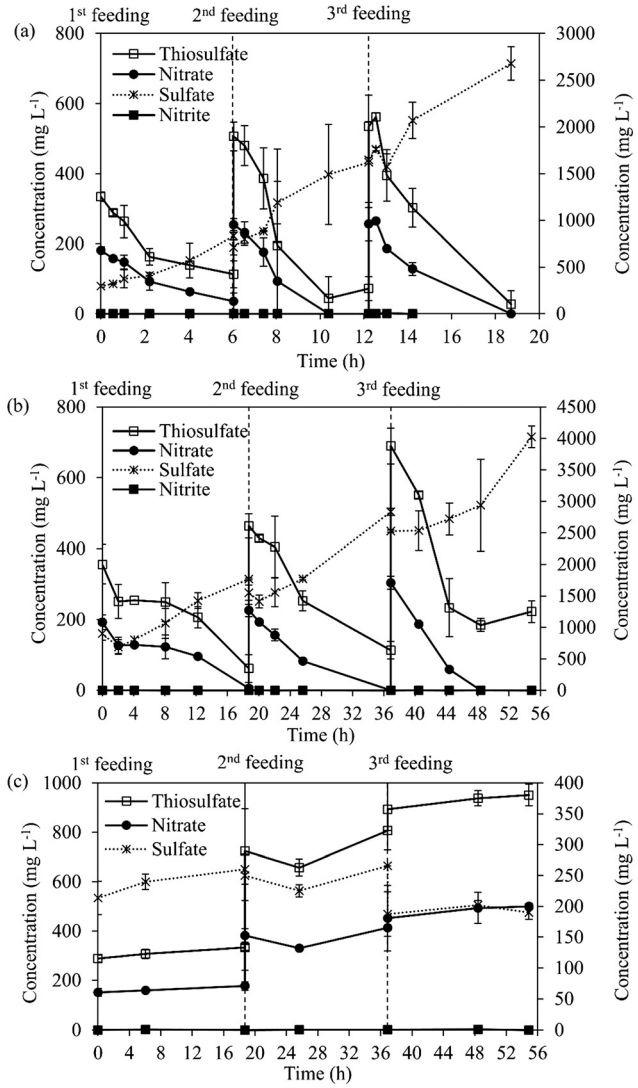

Fig. 4 Thiosulfate, nitrate, nitrite and sulfate concentrations during sequential feeding in batch bioassays performed with (a) carrier-attached biomass, (b) suspended biomass, and (c) without microorganisms (abiotic). Error bars represent the standard deviation.

3.5. Microbial community profile

The results of the PCR-DGGE analysis showed that the microbial community structure of the carrier-attached biomass changed during long-term MBBR operation (Fig. 6). The sequenced DGGE bands indicated that microorganisms having 97.6–99.6% similarity to *Thiobacillus* sp., *Chryseobacterium* sp., *Simplicispira* sp. and *Sulfuritalea* sp. were present in the MBBR biofilm during all the experimental periods. However, bands 9 and 11 related to a bacterium having 99.1–99.3% similarity to *T. denitrificans*, which were clearly visible in the DGGE profiles of periods I, III and IV, showed low intensity in period II. Bands 10 and 16, related to bacteria having 98.9 and 100% similarity to *Rhodocyclaceae* and *Thiomonas* sp., respectively, were detected in periods I, II and III but they faded away in period IV. Band 17, related to a bacterium with 99.3% similarity to *Desulfovibro* sp., was clearly detected in period III, whereas it had low intensity in periods I, II and IV.

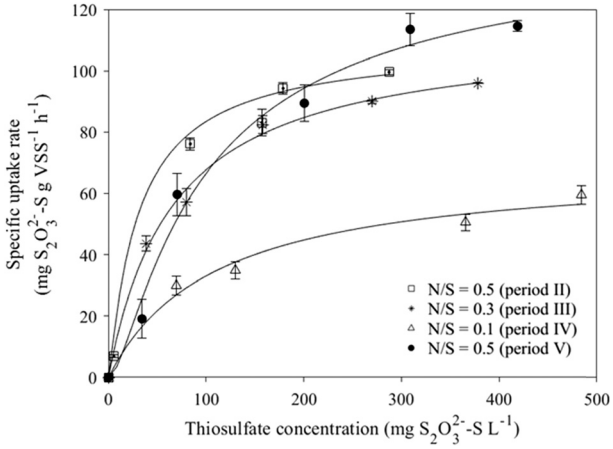

Fig. 5 Monod model prediction for estimating the maximum rate of sulfur oxidation (r_{max}) as well as $S_2O_3^{2-}$ (K_s) and NO_3^- (K_n) affinity constants of MBBR biomass collected at different N/S ratios. Dots and lines represent experimental and model fitted data, respectively. The error bars indicate the standard errors between the experimental and model fitted data.

Bands 7 and 8 had no significant similarities to the bacteria in the database due to the poor quality of the sequenced DNA. The microbial community composition of the suspended biomass samples was very similar to the carrier-attached communities during each operational period (data not shown).

4. Discussion

4.1. Effect of NO_3^- limitation on MBBR performance

The $S_2O_3^{2-}$ RE in the MBBR correlated with the NO_3^- loading rate (Fig. 2). Decreasing the NO_3^- concentration in the feed reduced the $S_2O_3^{2-}$ consumption and SO_4^{2-} production based on the stoichiometry described by eqn (1). The $S_2O_3^{2-}$ RE (Fig. 2c) during period V was higher than those observed in periods I and II, indicating that the sulfur-oxidizing capacity of the MBBR biofilm was enhanced after cultivation under severe NO_3^- limited conditions (N/S ratios of 0.3 and 0.1). In a previous work, the response of a sulfur-oxidizing FBR biofilm was investigated under the same NO_3^- limited conditions as applied in this study.[5] The $S_2O_3^{2-}$ RE of the FBR recovered to 80.8 (±4.1)% within 14 days after increasing the N/S ratio from 0.1 to 0.5. The MBBR operated in this study showed 8.2, 14.8 and 18.7% higher $S_2O_3^{2-}$ RE during operation at feed N/S ratios of 0.3, 0.1 and 0.5 (after severe NO_3^- limitation) and a much shorter recovery period (2 days) after restoring the N/S ratio from 0.1 to 0.5.[5] This was presumably due to the different bioreactor configuration used, microbial community structure as well as biomass and DO concentrations in the two reactors. The higher DO concentrations observed in the MBBR (0.45 mg L^{-1}) during the study compared to the condition maintained in the FBR (0.25 mg L^{-1}) likely stimulated bacteria capable of sulfur oxidation using the small amount of O_2 present in the MBBR biofilm, *i.e. Thiomonas* sp. and *Thiobacillus* sp.

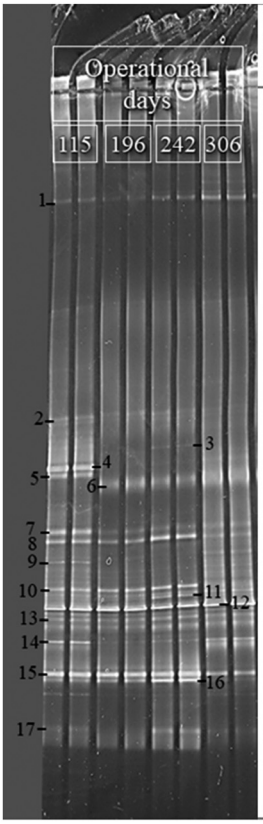

Band label	Affiliation	Class	Matching sequence length	Sequence ID	Similarity (%)
1	Uncultured bacterium clone LNH_9_9_11_Water.153675 16S ribosomal RNA gene		570	KM131698.1	100
2-3	*Flavobacteriaceae* bacterium	Flavobacteriales	410-434	EU642061.1	91.3-97.6
4-6	*Chryseobacterium* sp.	Flavobacteriales	451-526	EU706218.1	99.3-99.6
7	Uncultured bacterium partial 16S rRNA gene, isolate EFW618		463	LN889996.1	96.1
9, 11	*Thiobacillus denitrificans*	Betaproteobacteria	429-441	NR_025358.1	99.1-99.3
10	*Rhodocyclaceae* bacterium	Betaproteobacteria	434	FM207908.1	100
12	*Thiobacillus* sp.	Betaproteobacteria	458	KM595278.1	97.9
13	*Simplicispira* sp.	Betaproteobacteria	436	AB795522.1	98.6
14	Denitrifying bacterium	Betaproteobacteria	406	Y09967.1	93.9
15	*Sulfuritalea* sp.	Betaproteobacteria	488	JX493272.1	97.6
16	*Thiomonas* sp.	Betaproteobacteria	466	LN864654.1	98.9
17	*Desulfovibrio* sp.	Deltaproteobacteria	429	JX828422.1	99.3

Fig. 6 Polymerase chain reaction-denaturing gradient gel electrophoresis profiling of the microbial community composition of the K1 carrier-attached biomass in the MBBR during experimental periods II (day 115), III (day 196), IV (day 242) and V (day 306). Each sample was run in duplicate.

During this study, $S_2O_3^{2-}$ was oxidized to mainly SO_4^{2-} in all the operational conditions. The effluent SO_4^{2-} concentrations exceeded the theoretical values (calculated based on eqn (1)) throughout the study (Fig. 2c), being particularly high at the beginning of period I. The high SO_4^{2-} concentration observed in the MBBR effluent can be attributed to the oxidation of excess $S_2O_3^{2-}$ and other sulfur compounds formed in the system, *i.e.* H_2S and S^0. The biological disproportionation of excess $S_2O_3^{2-}$ to sulfide and SO_4^{2-} (according to eqn (6)) could also have occurred in the MBBR:

$$S_2O_3^{2-} + H_2O \rightarrow SO_4^{2-} + 0.5H_2S + 0.5HS^- + 0.5H^+ \quad \Delta G^0 = -25 \text{ kJ mol}^{-1} \quad (6)$$

Moreover, excess SO_4^{2-} production in the MBBR could be also produced by the complete oxidation of the biogenic S^0 accumulated intracellularly by the SO-NR bacteria during the previous long-term cultivation at extremely high $S_2O_3^{2-}$ concentrations and loading rates of the bioreactor used as an inoculum source.[6,17] NO_3^- limited conditions could promote partial $S_2O_3^{2-}$ oxidation to S^0 in the MBBR due to excess availability of electron donor compared to electron acceptor.[17] The S^0 disproportionation can be described by eqn (7):[23]

$$4S^0 + 4H_2O \rightarrow 3H_2S + SO_4^{2-} + 2H^+ \quad (7)$$

4.2. Effect of NO_3^- limited conditions on quantity and activity of the MBBR biomass

The MBBR showed good ability to develop a SO-NR biofilm, resulting in a VS/TS ratio up to 0.94 (Fig. 3). The affinity constant of the SO-NR biomass for $S_2O_3^{2-}$ (K_s = 1.7 mg $S_2O_3^{2-}$ L, at N/S ratio of 0.5) observed in period II (N/S ratio of 0.5) was lower than the values previously reported for sulfur-oxidizing biomass cultivated in other bioreactors, *i.e.* CSTR (16.1 mg $S_2O_3^{2-}$–S L^{-1}) and FBR (45.1 mg $S_2O_3^{2-}$–S L^{-1}).[5,24] The higher K_s observed at N/S ratios of 0.3 and 0.1 (Fig. 5) were clearly due to the cultivation under NO_3^- limitation.

This study also revealed that the active SO-NR biomass decreased during cultivation at a N/S ratio of 0.1 resulted in the lowest r_{max}. The metabolic activity of the SO-NR bacteria populating the MBBR biofilm was enhanced after cultivation under severely NO_3^- limited conditions (N/S ratio of 0.1), as the highest r_{max} was observed during period V (N/S ratio of 0.1). The NO_3^- limited conditions probably increased the amount of active SO-NR biomass during period V, as suggested by the higher affinity constants but similar biomass concentration compared to period II (N/S ratio of 0.5) (Table 2). Stress conditions such as nutrient limitation can induce a delay in biochemical conversions and enhance the production of extracellular polymeric substances (EPS), which serve as a supplementary substrate source and protect the bacterial cells from harmful toxic materials.[25] EPS overproduction can

increase the adhesive properties of the biofilm, enhancing its ability to withstand stress and harsh operating conditions.[26]

The results obtained from the sequential feeding experiment (Fig. 4, Table S1†) revealed that the suspended biomass in the MBBR could also remove $S_2O_3^{2-}$ and NO_3^- efficiently. As those sequential feedings resulted in an increase in the food to biomass ratio, *i.e.* higher substrate availability, an increase in the STUR and SNUR was observed for the suspended biomass. This observation is in agreement with the results of Reboleiro-Rivas *et al.*[27] who reported the utilization of high inlet organic loads with a lower biomass concentration in an aerobic moving bed membrane bioreactor treating municipal wastewater. In that study, the enzymatic activities, *i.e.* alkaline phosphatase, acid phosphatase and α-glucosidase activities, of the suspended biomass samples were higher than the activities observed in the attached biofilm samples due to better substrate diffusion. In biofilm reactors, fast-growing bacteria commonly grow in suspension, while the slow-growing bacteria aggregate to form a biofilm.[28] However, NO_3^- limited conditions (N/S ratios of 0.3 and 0.1) strongly reduced the suspended biomass concentration, which decreased from 200 mg VSS L^{-1} (period I) to less than 5 mg VSS L^{-1} (period IV) (Fig. 3). Conversely, the quantity of the attached growth biomass remained relatively constant after the acclimation period of the MBBR (day 90) (Fig. 3), which confirms the good resilience of the SO-NR biofilm to withstand NO_3^- limited conditions.

During the MBBR operation, the observed fine activated carbon particles attached on the surface of the K1 carriers (thick-dark brown biofilm, Fig. 1a) were able to maintain high and constant biomass quantity, particularly under severe NO_3^- limitation (Fig. 3). Similarly, several studies reported that the activated carbon powder provided an efficient surface for the attached biomass and increase the resistant effect of fluctuating loading of substrate enhanced biofilm.[29–31]

4.3. Effect of NO_3^- limited conditions on microbial community composition

The MBBR enabled to effectively maintain and enrich autotrophic SO-NR bacteria such as *Thiobacillus* sp., *T. denitrificans* and *Sulfuritalea* sp., as they were detected at all tested N/S ratios (Fig. 6). The growth of heterotrophic bacteria, such as *Thiomonas* sp., *Rhodocyclaceae* bacterium and *Chryseobacterium* sp., in the MBBR biofilm could be sustained by soluble microbial and cell lysis products (*e.g.* acetate, glucose and pyruvate) available under autotrophic conditions.[16,32,33] In particular, the reduction of biomass weight indicated that biofilm degradation and/or detachment of the outer layer of the biofilm occurred during period IV and were likely responsible for the enhanced growth of *Thiomonas*- and *Desulfovibrio*-like bacteria. *Desulfovibrio* are sulfate-reducing bacteria (SRB) commonly found in the inner parts of a biofilm which are also capable of disproportioning $S_2O_3^{2-}$ to H_2S and SO_4^{2-} (eqn (6) and (7)).[34,35]

5. Conclusions

The MBBR is a robust biofilm system for anoxic $S_2O_3^{2-}$ oxidation under severe NO_3^- limitation (feed N/S ratio 0.1). The SO-NR biofilm in the MBBR demonstrated high resiliency, being able to recover the $S_2O_3^{2-}$ RE from 37% to 94% within two days after increasing the feed N/S ratio from 0.1 to 0.5. The r_{max} and K_s of the SO-NR biofilm in the MBBR at a N/S ratio of 0.5 after severe NO_3^- limitation were 1.3-fold and 30-fold, respectively, higher than those observed at the same N/S ratio prior to cultivation at lower N/S ratios. Nevertheless, long-term operation at low N/S ratios reduced the amount of active SO-NR biomass in the system. Biomass sloughing due to long-term NO_3^- limitation supported the growth of heterotrophic bacteria in the MBBR.

Conflicts of interest

The authors declare no conflict of interest.

Acknowledgements

This research was supported by the Marie Skłodowska-Curie European Joint Doctorate (EJD) Advanced Biological Waste-To-Energy Technologies (ABWET) funded by the European Union's Horizon 2020 research and innovation programme [grant number 643071].

References

1 D. Pokorna and J. Zabranska, Sulfur-oxidizing bacteria in environmental technology, *Biotechnol. Adv.*, 2015, **33**, 1246–1259.
2 L. Krayzelova, J. Bartacek, I. Díaz, D. Jeison, E. I. P. Volcke and P. Jenicek, Microaeration for hydrogen sulfide removal during anaerobic treatment: A review, *Rev. Environ. Sci. Bio/Technol.*, 2015, **14**, 703–735.
3 F. Di Capua, S. H. Ahoranta, S. Papirio, P. N. L. Lens and G. Esposito, Impacts of sulfur source and temperature on sulfur-driven denitrification by pure and mixed cultures of Thiobacillus, *Process Biochem.*, 2016, **51**, 1576–1584.
4 M. Fernández, M. Ramírez, J. M. Gómez and D. Cantero, Biogas biodesulfurization in an anoxic biotrickling filter packed with open-pore polyurethane foam, *J. Hazard. Mater.*, 2014, **264**, 529–535.
5 R. Khanongnuch, F. Di Capua, A.-M. Lakaniemi, E. R. Rene and P. N. L. Lens, Effect of N/S ratio on anoxic thiosulfate oxidation in a fluidized bed reactor: experimental and artificial neural network model analysis, *Process Biochem.*, 2018, **68**, 171–181.
6 G. Zou, S. Papirio, A.-M. Lakaniemi, S. H. Ahoranta and J. A. Puhakka, High rate autotrophic denitrification in fluidized-bed biofilm reactors, *Chem. Eng. J.*, 2016, **284**, 1287–1294.
7 F. Di Capua, F. Pirozzi, P. N. L. Lens and G. Esposito, Electron donors for autotrophic denitrification, *Chem. Eng. J.*, 2019, **362**, 922–937.

8 B. Krishnakumar, S. Majumdar, V. B. Manilal and A. Haridas, Treatment of sulphide containing wastewater with sulphur recovery in a novel reverse fluidized loop reactor (RFLR), *Water Res.*, 2005, **39**, 639–647.

9 P. I. Cano, J. Colón, M. Ramírez, J. Lafuente, D. Gabriel and D. Cantero, Life cycle assessment of different physical-chemical and biological technologies for biogas desulfurization in sewage treatment plants, *J. Cleaner Prod.*, 2018, **181**, 663–674.

10 F. Di Capua, S. Papirio, P. N. L. Lens and G. Esposito, Chemolithotrophic denitrification in biofilm reactors, *Chem. Eng. J.*, 2015, **280**, 643–657.

11 M. Mora, A. Guisasola, X. Gamisans and D. Gabriel, Examining thiosulfate-driven autotrophic denitrification through respirometry, *Chemosphere*, 2014, **113**, 1–8.

12 S. Chai, J. Guo, Y. Chai, J. Cai and L. Gao, Anaerobic treatment of winery wastewater in moving bed biofilm reactors, *Desalin. Water Treat.*, 2014, **52**, 1841–1849.

13 S. N. H. Abu Bakar, H. Abu Hasan, A. W. Mohammad, S. R. S. Abdullah, T. Y. Haan, R. Ngteni and K. M. M. Yusof, A review of moving-bed biofilm reactor technology for palm oil mill effluent treatment, *J. Cleaner Prod.*, 2017, **171**, 1532–1545.

14 Q. Yuan, H. Wang, Q. Hang, Y. Deng, K. Liu, C. Li and S. Zheng, Comparison of the MBBR denitrification carriers for advanced nitrogen removal of wastewater treatment plant effluent, *Environ. Sci. Pollut. Res.*, 2015, **22**, 13970–13979.

15 W. Yang, J. Vollertsen and T. Hvitved-Jacobsen, Anoxic sulfide oxidation in wastewater of sewer networks, *Water Sci. Technol.*, 2005, **52**, 191–199.

16 F. Di Capua, A.-M. Lakaniemi, J. A. Puhakka, P. N. L. Lens and G. Esposito, High-rate thiosulfate-driven denitrification at pH lower than 5 in fluidized-bed reactor, *Chem. Eng. J.*, 2017, **310**, 282–291.

17 F. Di Capua, I. Milone, A.-M. Lakaniemi, P. N. L. Lens and G. Esposito, High-rate autotrophic denitrification in a fluidized-bed reactor at psychrophilic temperatures, *Chem. Eng. J.*, 2017, **313**, 591–598.

18 J. Luo, G. Tian and W. Lin, Enrichment, isolation and identification of sulfur-oxidizing bacteria from sulfide removing bioreactor, *J. Environ. Sci.*, 2013, **25**, 1393–1399.

19 L. Kopec, A. Kopec and J. Drewnowski, The application of Monod equation to denitrification kinetics description in the moving bed biofilm reactor (MBBR), *Int. J. Environ. Sci. Technol.*, 2018, 1–8.

20 H. S. Fogler, *Elements of chemical reaction engineering*, Prentice Hall, Indiana, 5th edn, 2016.

21 S. H. Ahoranta, M. E. Kokko, S. Papirio, B. Özkaya and J. A. Puhakka, Arsenic removal from acidic solutions with biogenic ferric precipitates, *J. Hazard. Mater.*, 2016, **306**, 124–132.

22 APHA/AWWA/WEF (American Public Health Association/American Water Works Association/Water Environment Federation), *Standard methods for the examination of water and wastewater*, APHA/AWWA/WEF, Washington D.C., 20th edn, 1999.

23 K. Finster, W. Liesack and B. Thamdrup, Elemental sulfur and thiosulfate disproportionation by *Desulfocapsa sulfoexigens* sp. nov., a new anaerobic bacterium isolated from marine surface sediment, *Appl. Environ. Microbiol.*, 1998, **64**, 119–125.

24 M. Mora, A. D. Dorado, X. Gamisans and D. Gabriel, Investigating the kinetics of autotrophic denitrification with thiosulfate: Modeling the denitritation mechanisms and the effect of the acclimation of SO-NR cultures to nitrite, *Chem. Eng. J.*, 2015, **262**, 235–241.

25 M. R. Chénier, D. Beaumier, R. Roy, B. T. Driscoll, J. R. Lawrence and C. W. Greer, Impact of seasonal variations and nutrient inputs on nitrogen cycling and degradation of hexadecane by replicated river biofilms, *Appl. Environ. Microbiol.*, 2013, **69**, 5170–5177.

26 T. R. Garrett, M. Bhakoo and Z. Zhang, Bacterial adhesion and biofilms on surfaces, *Prog. Nat. Sci.*, 2008, **18**, 1049–1056.

27 P. Reboleiro-Rivas, J. Martín-Pascual, B. Juárez-Jiménez, J. M. Poyatos, E. Hontoria, B. Rodelas and J. González-López, Enzymatic activities in a moving bed membrane bioreactor for real urban wastewater treatment: Effect of operational conditions, *Ecol. Eng.*, 2013, **61**, 23–33.

28 R. Nogueira, L. F. Melo, U. Purkhold, S. Wuertz and M. Wagner, Nitrifying and heterotrophic population dynamics in biofilm reactors: effects of hydraulic retention time and the presence of organic carbon, *Water Res.*, 2002, **36**, 469–481.

29 G. Skouteris, D. Saroj, P. Melidis, F. I. Hai and S. Ouki, The effect of activated carbon addition on membrane bioreactor processes for wastewater treatment and reclamation - A critical review, *Bioresour. Technol.*, 2015, **185**, 399–410.

30 Y. C. Woo, J. J. Lee, W. G. Shim, H. K. Shon, L. D. Tijing, M. Yao and H. S. Kim, Effect of powdered activated carbon on integrated submerged membrane bioreactor-nanofiltration process for wastewater reclamation, *Bioresour. Technol.*, 2016, **210**, 18–25.

31 B. E. L. Baêta, R. L. Ramos, D. R. S. Lima and S. F. Aquino, Use of submerged anaerobic membrane bioreactor (SAMBR) containing powdered activated carbon (PAC) for the treatment of textile effluents, *Water Sci. Technol.*, 2012, **65**, 1540–1547.

32 R. Khanongnuch, F. Di Capua, A.-M. Lakaniemi, E. R. Rene and P. N. L. Lens, H_2S removal and microbial community composition in an anoxic biotrickling filter under autotrophic and mixotrophic conditions, *J. Hazard. Mater.*, 2018, **367**, 397–406.

33 Y. Wang, C. Bott and R. Nerenberg, Sulfur-based denitrification: Effect of biofilm development on denitrification fluxes, *Water Res.*, 2016, **100**, 184–193.

34 J. Qian, H. Lu, Y. Cui, L. Wei, R. Liu and G. H. Chen, Investigation on thiosulfate-involved organics and nitrogen removal by a sulfur cycle-based biological wastewater treatment process, *Water Res.*, 2015, **69**, 295–306.

35 F. Di Capua, I. Milone, A.-M. Lakaniemi, E. D. va. Hullebusch, P. N. L. Lens and G. Esposito, Effects of different nickel species on autotrophic denitrification driven by thiosulfate in batch tests and a fluidized-bed reactor, *Bioresour. Technol.*, 2017, **238**, 534–541.